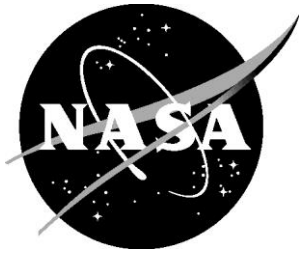


NASA/TM-2016-219175



# ATD Occupant Responses from Three Full-Scale General Aviation Crash Tests

*Justin D. Littell and Martin S. Annett  
Langley Research Center, Hampton, Virginia*

---

March 2016

## NASA STI Program . . . in Profile

Since its founding, NASA has been dedicated to the advancement of aeronautics and space science. The NASA scientific and technical information (STI) program plays a key part in helping NASA maintain this important role.

The NASA STI program operates under the auspices of the Agency Chief Information Officer. It collects, organizes, provides for archiving, and disseminates NASA's STI. The NASA STI program provides access to the NTRS Registered and its public interface, the NASA Technical Reports Server, thus providing one of the largest collections of aeronautical and space science STI in the world. Results are published in both non-NASA channels and by NASA in the NASA STI Report Series, which includes the following report types:

- **TECHNICAL PUBLICATION.** Reports of completed research or a major significant phase of research that present the results of NASA Programs and include extensive data or theoretical analysis. Includes compilations of significant scientific and technical data and information deemed to be of continuing reference value. NASA counter-part of peer-reviewed formal professional papers but has less stringent limitations on manuscript length and extent of graphic presentations.
- **TECHNICAL MEMORANDUM.** Scientific and technical findings that are preliminary or of specialized interest, e.g., quick release reports, working papers, and bibliographies that contain minimal annotation. Does not contain extensive analysis.
- **CONTRACTOR REPORT.** Scientific and technical findings by NASA-sponsored contractors and grantees.

- **CONFERENCE PUBLICATION.** Collected papers from scientific and technical conferences, symposia, seminars, or other meetings sponsored or co-sponsored by NASA.
- **SPECIAL PUBLICATION.** Scientific, technical, or historical information from NASA programs, projects, and missions, often concerned with subjects having substantial public interest.
- **TECHNICAL TRANSLATION.** English-language translations of foreign scientific and technical material pertinent to NASA's mission.

Specialized services also include organizing and publishing research results, distributing specialized research announcements and feeds, providing information desk and personal search support, and enabling data exchange services.

For more information about the NASA STI program, see the following:

- Access the NASA STI program home page at <http://www.sti.nasa.gov>
- E-mail your question to [help@sti.nasa.gov](mailto:help@sti.nasa.gov)
- Phone the NASA STI Information Desk at 757-864-9658
- Write to:  
NASA STI Information Desk  
Mail Stop 148  
NASA Langley Research Center  
Hampton, VA 23681-2199

NASA/TM-2016-219175



# ATD Occupant Responses from Three Full-Scale General Aviation Crash Tests

*Justin D. Littell and Martin S. Annett  
Langley Research Center, Hampton, Virginia*

National Aeronautics and  
Space Administration

Langley Research Center  
Hampton, Virginia 23681-2199

---

March 2016

The use of trademarks or names of manufacturers in this report is for accurate reporting and does not constitute an official endorsement, either expressed or implied, of such products or manufacturers by the National Aeronautics and Space Administration.

Available from:

NASA STI Program / Mail Stop 148  
NASA Langley Research Center  
Hampton, VA 23681-2199  
Fax: 757-864-6500

## **Abstract**

During the summer of 2015, three Cessna 172 General Aviation (GA) aircraft were crash tested at the Landing and Impact Research (LandIR) Facility at NASA Langley Research Center (LaRC). Three different crash scenarios were represented. The first test simulated a flare-to-stall emergency or hard landing onto a rigid surface such as a road or runway. The second test simulated a controlled flight into terrain with a nose down pitch of the aircraft, and the third test simulated a controlled flight into terrain with an attempt to unsuccessfully recover the aircraft immediately prior to impact, resulting in a tail strike condition. An on-board data acquisition system (DAS) captured 64 channels of airframe acceleration, along with accelerations and loads in two onboard Hybrid II 50<sup>th</sup> percentile Anthropomorphic Test Devices (ATDs) representing the pilot and co-pilot. Each of the three tests contained different airframe loading conditions and different types of restraints for both the pilot and co-pilot ATDs. The results show large differences in occupant response and restraint performance with varying likelihoods of occupant injury.

## Introduction

During the summer of 2015, three full-scale crash tests of Cessna 172 aircraft were conducted at NASA Langley Research Center's (LaRC) Landing and Impact Research (LandIR) Facility. These crash tests were conducted as a part of the Emergency Locator Transmitter Survivability and Reliability (ELTSAR) project, which had the ultimate goal of improving Emergency Locator Transmitter (ELT) reliability [1]. The LandIR facility has been in use since the mid 1970's to conduct full-scale crash tests on aircraft and spacecraft for the improvement of safety features [2]. LandIR is a unique facility that is used to impart combined forward and vertical velocities onto test articles at complex impact attitudes, which create more realistic crash conditions and scenarios than those tests conducted by pure vertical drops. The facility uses a pendulum-like swing system to lift and swing the test articles into the ground. Pitch rate can be varied or eliminated and the facility is capable of lifting and swinging test articles up to 32 tons in weight. Combinations of swing cable length, drop height, angle of attack, impact surface (rigid, soil or water) and location can all be varied, creating a wide range of impact conditions.

Some of the many full-scale tests conducted at LandIR led to improvements in seat certification guidelines [3], the development of parachute recovery system [4], and the development of composite crashworthiness airframe features [5]. The facility continues to provide critical safety research for the aviation community. The LandIR facility is shown in Figure 1.



Figure 1 - Landing and Impact Research Facility (LandIR)

The three tests Cessna 172 conducted were intended to represent general aviation (GA) accidents in which the airplane impacts the ground under severe but survivable conditions. A severe but survivable crash condition is of interest for the ELTSAR project because ELT systems must function in a mishap where the occupants are physically incapacitated but alive and unable to call for help. A severe but survivable crash condition is also preferable because it will quantitatively define (in part) the limits in which an occupant is reasonably expected to be able to survive the crash. In order to help quantify the severity of the crash, airframe accelerations and post-test deformation were all examined, and two Anthropomorphic Test Devices (ATDs, a.k.a. crash test dummies) representing the pilot and co-pilot were used in each test. The main objective for using the ATDs was to measure loads and accelerations within the ATD head, chest, pelvis and lumbar region, and to compare the data to established injury metrics and limits to determine the probability and severity of injury.

Aircraft accidents, unfortunately, have a part of the aviation community ever since people have been flying airplanes. The National Transportation Safety Board (NTSB) reports that between 1972 and 1981, there were over 36,000 accidents involving GA aircraft. From these, 16% included fatalities, and 9% included serious injuries [6]. A more recent NTSB summary from 2002 shows fatal accident rates have remained mostly constant between the years of 1993 (3.3 deaths per 100,000 hours flown) and 2002 (2.3 deaths per 100,000 hours flown) [7]. Even with improvements constantly being made in aircraft crashworthiness, the persistence of accident occurrences in GA shows that research is still necessary for implementing guidelines for improvements in aircraft, seat and restraint performance.

In one notable example, the Federal Aviation Administration (FAA) Code of Federal Regulations (CFR) Section 23.2, “Special Retroactive Requirements,” has mandated that shoulder harnesses must be provided on all airplanes manufactured after December 12, 1986 [8]. Literature has already shown that the use of a shoulder harness has significantly reduced fatality rates during aircraft accidents. One study conducted on commuter and air taxi crashes suggests that the use of a shoulder harness reduces the chances of fatality by a factor of almost 4 [9], and the FAA states that using shoulder belts in small aircraft would reduce major injuries by 88% and fatalities by 20% [10]. Similarly, the Canadian Transportation Safety Administration (TSA) states “the use of a shoulder harness in conjunction with a safety belt can reduce serious injuries to the head, neck, and upper torso of aircraft occupants and has the potential to reduce fatalities of occupants involved in an otherwise survivable accident [11].” Additionally, restraint systems containing airbags were first certified in 2003 by the FAA and have been proven successful in reducing the severity of occupant injury, according to one NTSB study [12].

Crash testing can be used to assess injury through the simulation of real life conditions by using flight or flight-like structures and ATDs. This type of testing is often superior to actual crash data due to the controlled conditions used in crash testing and rigor used in data collection. In most instances, the acquisition of accident data is obtained through mishap reports, and databases containing parameters of the crash (make/model of airplane, impact conditions, weather, etc.) are in many cases incomplete and often subject to interpretation. Subcomponent tests, such as the FAA seat qualification tests [3], are a tier below full-scale experimentation, but nonetheless provide controlled conditions for which to evaluate components. NASA has conducted many full-

scale and subscale crash tests under a variety of conditions, using instrumented ATDs and various airframes and airframe components. Many of the airframe and occupant injury data for both helicopters [13-16] and airplanes [17] has been published. By using the crash test data obtained during the Cessna 172 crash tests, along with established injury criteria, a complete analysis of the crash severity can be obtained and used to further understand real life accidents.

## **Crash Test Overview**

Three Cessna 172 airplanes were used as test articles. Airplanes used for Tests 1 and 2 were a 1958 model year, while the airplane used for Test 3 was a 1974 model year. Airplanes 1 and 3 were current on their annual inspection and were flying as of late 2014. Three differing accidents representing severe but survivable crash scenarios were evaluated for the test series. The first scenario represented a flare-into-stall emergency landing onto a rigid surface such as a highway. This scenario was tested by impacting the airplane onto concrete featuring a high sink rate at a slight nose up attitude. The second and third scenarios were impact tests onto a soil surface. This surface was created by building up a 2-ft. high bed of soil at the impact location. In scenario two, the airplane impacted the soil in a nose down attitude, simulating a Controlled Flight Into Terrain (CFIT). In the third scenario, the airplane impacted the soil in a nose up attitude, resulting in a tail strike condition.

Each airplane was outfitted with numerous accelerometers and cameras which captured as much of the impact accelerations and structural deformation as possible. The pilot side of the airplane was painted with a stochastic black and white speckle pattern which was used for full field photogrammetric tracking and is the subject of a separate report [18]. Each test contained two Hybrid II 50<sup>th</sup> percentile ATDs, which represented the pilot and co-pilot.

Each ATD was restrained using commonly used restraints in typical GA airplanes. The restraints were intentionally varied between the pilot and co-pilot for each test to provide comparative results and probability of injury for different restraints. Furthermore, restraint types varied between tests, giving a total of six discrete data points to evaluate. One major objective of varying the restraint types was to generate data of occupant responses when using various types of 3-point shoulder harnesses as compared to a 2-point lap belt only restraint.

The original seats for all three airplanes were used. The ATD occupants were positioned such that their feet contacted the brake pedals and hands were placed on their knees. All restraint systems were purchased new and installed per manufacturer's instructions. On airplanes which did not include anchoring locations of the restraints due to model year, a retrofit kit included with the restraint was installed according to manufacturer's instructions. Details describing the specific types of restraints are provided in each of the following test sections. Once tested, restraints were not reused. Each ATD was instrumented with 7 channels of data and all instrumentation was oriented to and all results were filtered in accordance to SAE-J211 [19]. These channels are summarized in Table 1.



Table 1 – ATD instrumentation

ATD Location	Measurement	Direction
Head	Acceleration	Horizontal, Vertical
Chest	Acceleration	Horizontal
Pelvis	Acceleration	Horizontal, Vertical
Lumbar	Force	Vertical
Seatbelt	Force	Strap tension

Full details describing each test, along with airframe results, time histories and photos are provided in [20]; however, some of the results from each test are summarized herein.

## Test 1 Results

Test 1 occurred on July 1, 2015, and simulated an emergency landing onto a rigid surface such as concrete or a highway. The airplane center of gravity (CG) impacted the ground at a flight path velocity of 64.4 ft./sec., corresponding to 60.2-ft./sec. horizontal and 23.0-ft./sec. vertical velocities at an Angle of Attack (AoA) of 1.5 degrees nose high. The landing gear compressed for approximately 0.300 seconds and the plane rebounded from the ground with a large amount of residual horizontal velocity and then contacted a large catch net approximately 0.475 seconds after impact. The large catch net was the main mechanism for providing the horizontal deceleration. The accelerations throughout the entire airframe were in general agreement with each other, and are fully described and plotted in [20]. Accelerations measured by accelerometers mounted beneath both the pilot and co-pilots seats, generally agreed with the other airframe accelerations, and are shown in Figure 2.

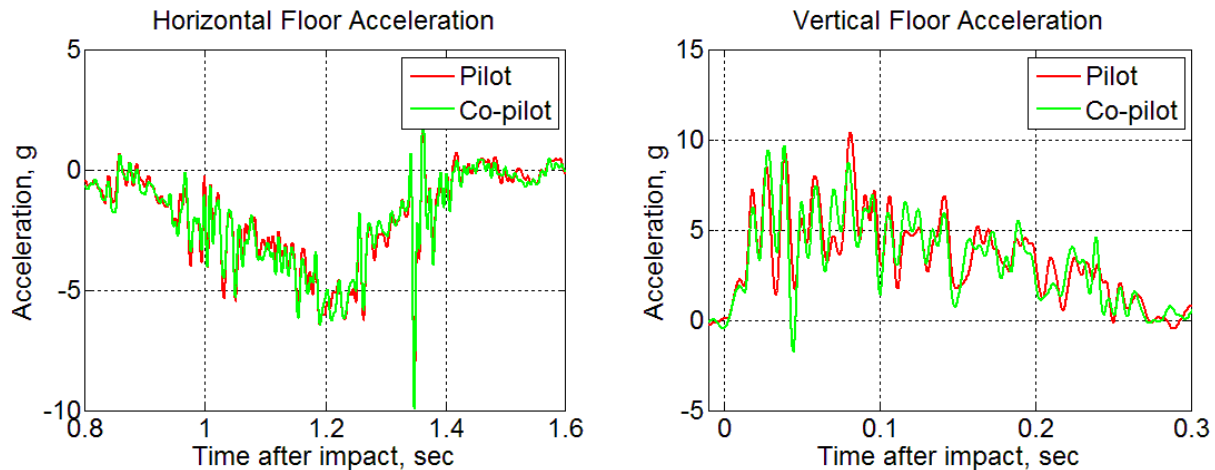


Figure 2 - Floor accelerations from Test 1

The peak vertical floor accelerations mainly occurred during the first 0.300 seconds after initial ground contact. The shape of the pulse can be generalized as trapezoidal in nature, having a

sustained average acceleration of 4.8 g for the pilot and 4.6 g for the co-pilot. The trapezoidal shape is sustained from the landing gear flexing. Horizontal accelerations were mainly seen during the post-impact net capture, which occurred between 0.800 seconds and 1.600 seconds after initial ground impact. The shape of the horizontal acceleration pulse was generalized as triangular, having peaks of 5.4 g for both the pilot and co-pilot, which occurred approximately 1.200 seconds after impact, or during the middle of the net capture event. When examining occupant motion and accelerations, it generally follows that the relevant occupant vertical motion occurs due to the ground contact, and the relevant occupant horizontal motion occurs due to the net capture.

The pilot was outfitted with a 3 point restraint, consisting of a fixed lap and shoulder belt. The co-pilot was outfitted with a lap belt only. Figure 3 shows the pre-test setup for the occupants for Test 1. Note since the co-pilot was not wearing a shoulder belt, he was taped into the seat to prevent slouching forward during airplane pullback, prior to impact. The tape was designed to fail upon ground impact.



Figure 3 - Test 1 ATD configuration pre-test

An onboard high speed camera mounted in the instrument panel was able to capture the entire impact event, starting at ground contact and ending after the net capture. Four frames of the video are presented in Figure 4. The four frames represent notable event times from either the occupant or the restraint. The photo shown in the upper left corner shows the occupants immediately before impact, indicating symmetric positioning between the pilot and co-pilot, with the exception that the co-pilot's right hand becomes dislodged from its original location on the right knee. The frame in the upper right shows the approximate time in which the occupants experienced the maximum lumbar load, which occurred very early in the ground contact at 0.076 seconds after impact. The occupants do not show noticeable forward displacement, and only a slight amount of vertical deformation into the seats. The frame in the lower left shows the time at which the restraint load cell measured maximum tensile load, which occurred at the same approximate time of maximum horizontal deceleration due to the net capture. The lower right frame shows the occupant position, after the airplane motion has stopped. Figure 5 shows the same image sequence taken from the pilot wing camera.

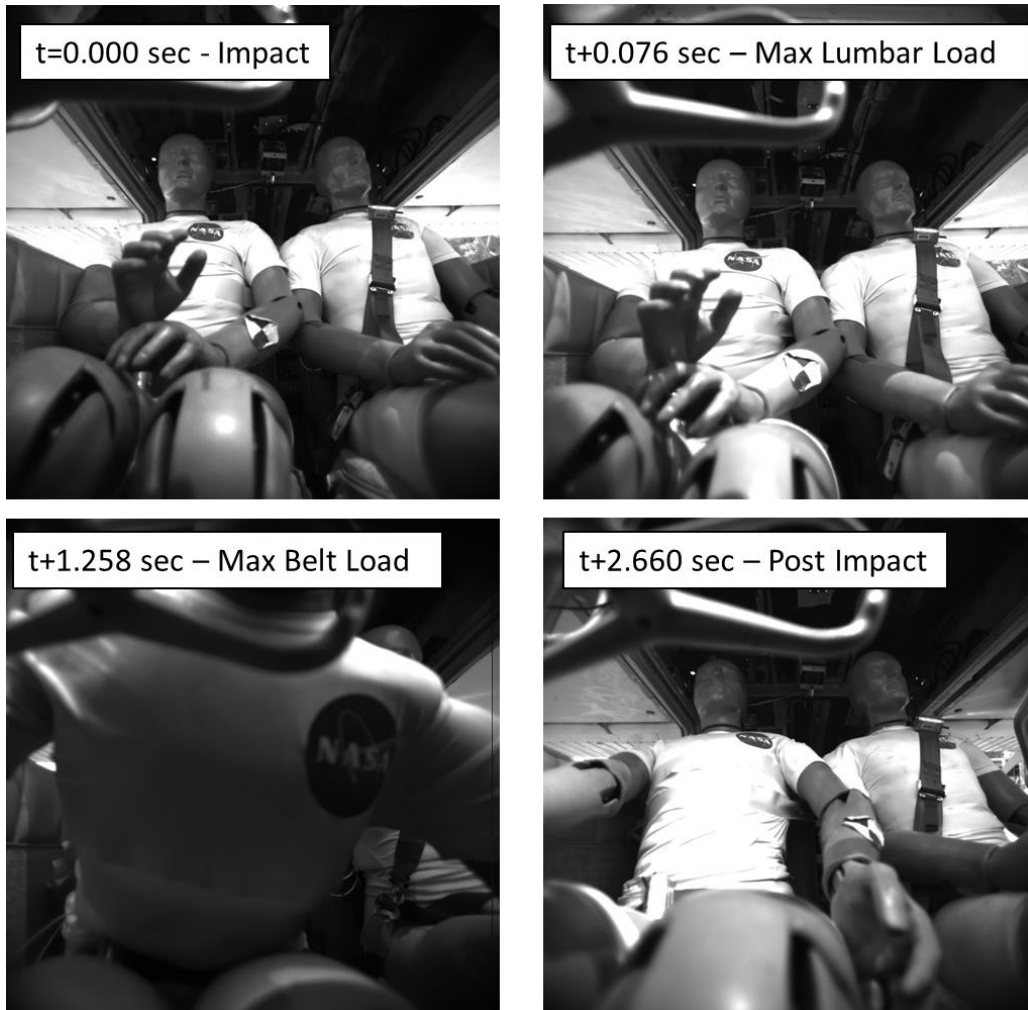


Figure 4 - Test 1 occupant motion sequence - onboard camera

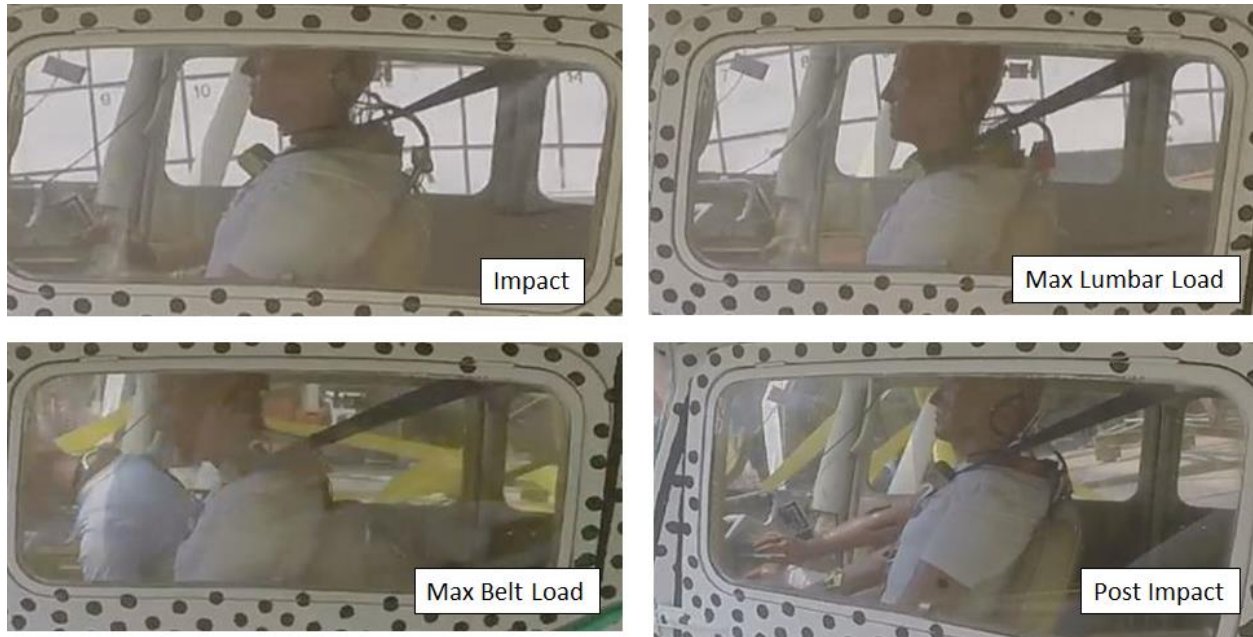


Figure 5 - Test 1 occupant sequence - wing camera

The vertical displacement causing the maximum lumbar load in the occupants is evident from the wing camera. Noticeable vertical displacement is present in both the pilot and co-pilot causing the lumbar load to reach a maximum value. The camera also showed noticeable differences in the position of the head and chest during the time of maximum belt load. The post impact image shows that the occupants generally return to their pre-impact position.

Maximum head flail was further examined for both the pilot and co-pilot. The maximum head flail for the pilot occurred at 1.063 seconds after impact, while the maximum head flail for the co-pilot occurred a short time later at 1.132 seconds after impact. Both of these events occurred from the horizontal deceleration due to the net catch. Figure 6 and Figure 7 show the closest available frame taken from the wing cameras for the pilot and co-pilot, respectively, and compared them to a pre-impact state. Using the best available scaling information based on the known size of the window, the pilot's head experienced slightly less than 4 in. of forward travel. Using the best available scaling information based on the known size of the co-pilot window, the large amount of motion of the co-pilot head achieved a maximum forward displacement of approximately 17 in. when compared to the head prior to impact.



Figure 6 – Test 1 pilot head flail. Before impact (top) and max flail (bottom)





Figure 7 - Test 1 co-pilot head flail. Before impact (top) and at max flail (bottom)

The type of restraint clearly affected the maximum head motion. The addition of the shoulder belt reduced the head motion by approximately 13 in. and clearly prevented the pilot from striking the instrument panel. However, it was unclear from both the wing and the panel video as to whether the co-pilot head had actually made contact with the instrument panel. The acceleration responses from the head are next plotted to obtain insight into the ATD accelerations and loads. Figure 8 first shows the ATD horizontal accelerations.

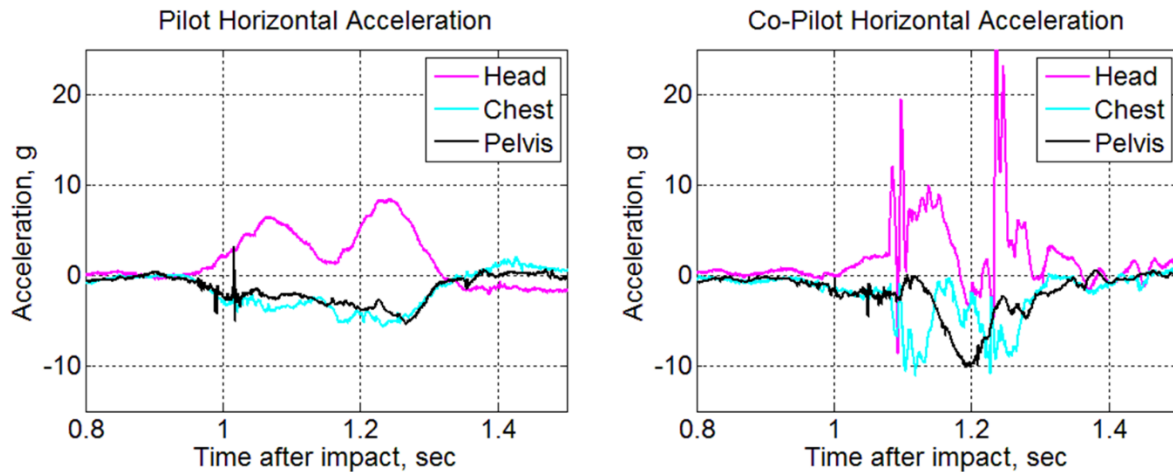


Figure 8 - Test 1 ATD horizontal acceleration. Pilot (left) and co-pilot (right)

As stated previously, since the majority of the horizontal accelerations occurred during the net catch event, the accelerations in the occupants will be examined during the net catch. Generally, the pilot and co-pilot accelerations match shape and duration in the horizontal direction. The pilot acceleration signal shows a smoother trace than the co-pilot, and the co-pilot seems to experience at least two minor spikes in head acceleration. The pilot acceleration reaches maximums of 8.4, -5.6 and -5.3 g in the head, chest and pelvis, respectively. These results are contrasted in the co-pilot, which experiences 30.4 (not shown), -10.8 and -9.8 maximum g in the head, chest and pelvis, respectively. The larger peak value in the head could be due to an impact with either the yoke or instrument panel, while the large values in the chest and pelvis are likely due to the increased acceleration as the lap belt is loaded. Vertical acceleration is next examined, and shown in Figure 9.

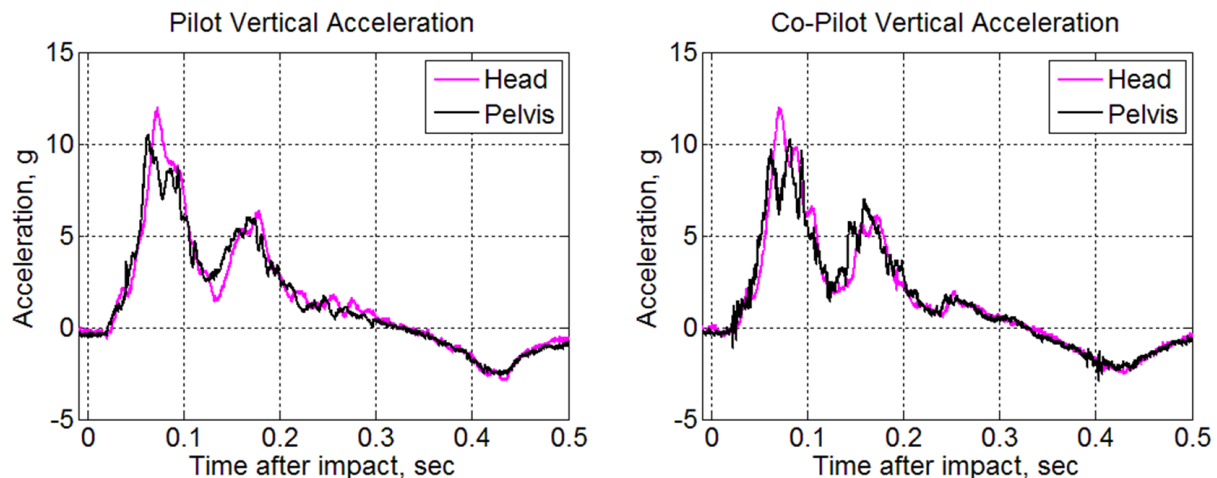


Figure 9 - Test 1 ATD vertical acceleration. Pilot (left) and co-pilot (right)

Using the data from the initial ground contact where the vertical accelerations are the most pronounced, the vertical accelerations for the pilot and co-pilot are in good agreement with each other. First examining the head, the maximum acceleration for both the pilot and co-pilot is 12.0 g, which occurs at 0.073 seconds after impact for the pilot and 0.07 seconds after impact for the co-pilot. The pelvic accelerations are slightly different, where the maximum acceleration for the pilot is 10.5 g and the maximum for the co-pilot is 10.3 g. The pulse durations for the head and pelvis match each other for both the pilot and co-pilot, as do the pulse durations. These results indicate uniform loading, which is a result of the initial vertical impact. The data were next used to calculate a Head Injury Criteria value.

Head injury criteria (HIC), as defined in the Federal Motor Vehicle Safety Standards (FMVSS) No. 208 [21], is a way of evaluating the acceleration data obtained from an ATD during a crash test and equating it to the probability of skull fracture. The equation is:

$$HIC = \max \left( \frac{1}{t_2 - t_1} \int_{t_1}^{t_2} a(t) * dt \right)^{2.5} * (t_2 - t_1)$$

The variable  $a(t)$  is the root sum square of the head acceleration time history obtained from the test, which has moving end points of  $t_1$  and  $t_2$ . Typically, HIC uses a 36 millisecond moving window and a limit of 1000 for a 50<sup>th</sup> percentile ATD. The HIC value of 1000 gives the probability of a skull fracture (Abbreviated Injury Scale  $\geq 2$ ) at 48% [22], and is used as the limit in FAR 23.562 [23]. The HIC values for Test 1 are shown in Table 2.

Table 2 - Test 1 HIC36 values

	HIC36
Pilot	11
Co-pilot	25

As indicated in Table 2, neither the pilot nor co-pilot sustained high HIC loading from the test, suggesting that the co-pilot head did not strike the instrument panel. The acceleration profile from the net capture was low enough and spread over a large enough time period that both the spike magnitude and duration seen in the co-pilot head accelerations used for HIC did not register high enough values to cross the injurious threshold.

The tension developed in the restraints were next examined and plotted in Figure 10. The tension is measured on the pilot shoulder belt, while the tension is measured on the co-pilot lap belt due to the lack of a shoulder restraint.





Figure 10 - Test 1 restraint loads

The maximum restraint load of 491 lb. occurred at 1.26 seconds after ground contact for the pilot, and the maximum load of 294 lb. occurred at 1.18 seconds after ground contact for the co-pilot. Both of these times were during the horizontal deceleration due to the net capture. While not directly comparable due to differing measurement locations and differing restraint types, it is clear that the shoulder belt required almost 500 lb. of tension to restrain the pilot into the seat with a maximum head displacement of 4 in. Because the shoulder belt was not present in co-pilot, the main restraint was the lap belt, providing almost 300 lb. of tension to restrain the co-pilot into the seat near the co-pilot's pelvic region. The load measured in the pilot shoulder belt was below the 1,750 value specified in the FAR 23.562 [23].

Lumbar loads were next examined to check for spinal compression injury. Primarily vertical in nature, the main portion of the lumbar loads occurred during the initial ground contact where the highest vertical accelerations also occurred. The lumbar load was minimal during the net capture. Figure 11 shows the measured lumbar loads which occurred during the ground contact.

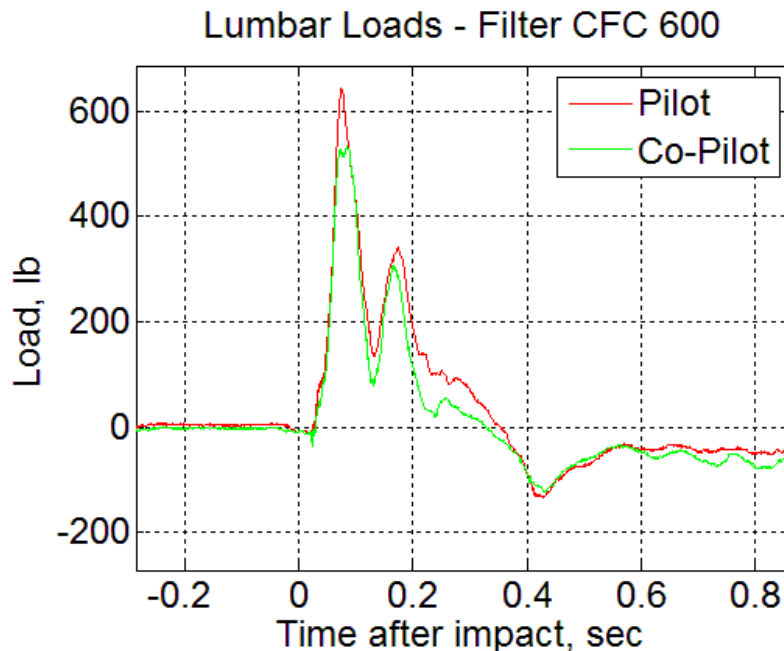


Figure 11 - Test 1 lumbar loads

The pilot lumbar load peaks at 643 lb., while the co-pilot lumbar load shows a peak value of 535 lb., both reaching peaks approximately 0.076 seconds after impact, which was near the beginning of the sustained portion in trapezoidal vertical acceleration profile. The approximate 100 lb. difference could be due to the addition of a shoulder restraint, slight differences in ATD positioning, or the seats themselves. However, both of these values are well below the 1,500 lb. limit established by the FAA in FAR 23.562 [23], indicating spinal compressive fracture likely did not occur.

The summary of Test 1 suggests that occupant loading from the ground contact caused accelerations and loads which were well below the established limits for injury. The co-pilot head accelerations suggest that the head may have hit the instrument panel; however, the deceleration due to the net catch was slow enough such that the head contact with the instrument panel was likely not fatal. The differences between using a shoulder with lap belt and a lap belt only are very evident during the large horizontal deceleration due to the net capture when comparing the torso flail between the pilot and co-pilot.

## Test 2 Results

Test 2 was conducted on July 29, 2015 and was the first of 2 tests where the airplane impacted a soil surface. The surface was to represent a dirt field or other type of unprepared surface not considered rigid. The airplane CG impacted the soil at a 68.6-ft./sec. horizontal and 28.7-ft./sec. vertical velocities. The AoA was 12.2 degrees nose down with a pitch rate of +16.1 degrees/second.

The nose of the airplane first came in contact with the soil due to the nose down configuration of the impact. While the nose and nose gear began plowing into the soil, the forward momentum

caused the airplane to start rotating about the nose/nose gear position, which acted like a pivot point from which to rotate. The airplane started to flip over, which caused the pilot wing to break free and also the tail to buckle. At some point during the flipping rotation, the nose wheel became dislodged from the airframe. The airplane landed upside down almost 2 seconds after impact, and rocked back and forth. Approximately 6.79 seconds after impact, the airplane came to rest, upside down and oriented toward the co-pilot direction. Figure 12 shows the post-crash orientation of the airplane.



Figure 12 - Post-test orientation of airplane in Test 2

Accelerations from accelerometers mounted on the floor under the crew seats are plotted in Figure 13. Unlike Test 1, both the main horizontal and vertical accelerations occurred within the first 0.300 seconds of ground (soil) contact.

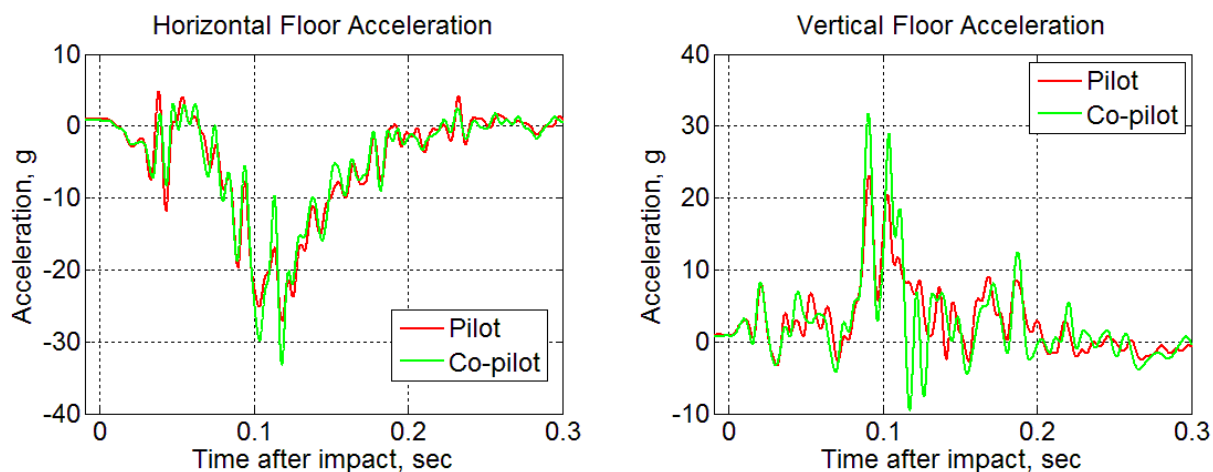


Figure 13 - Floor accelerations from Test 2

The horizontal acceleration pulse shapes were triangular having peak accelerations of -27.0 g for the pilot floor and -32.9 g for the co-pilot floor. The sustained peak value, which represented an

average value of the accelerations which occurred between 0.100 and 0.120 seconds was -18.6 g for both the pilot and co-pilot locations. The main horizontal acceleration pulse lasted for approximately 0.200 seconds after soil contact. The vertical acceleration was also triangular in shape, having peaks of 23.1 g in the pilot floor and 31.7 g in the co-pilot floor. The sustained peaks, taking the average between 0.086 and 0.11 seconds, gives 14.6 g and 17.6 g for the pilot and co-pilot, respectively. The pulse duration is much shorter than the horizontal pulse, with the main acceleration occurring between 0.0725 and 0.150 seconds, giving a total duration of 0.0775 seconds.

The pilot was outfitted with a lap belt only while the co-pilot was outfitted with a lap belt and shoulder y-harness. Both restraints were purchased new and outfitted into the existing restraint attachment points. For the shoulder y-harness, a retrofit kit was included and installed per manufacturer's instructions, which required the y-harness to attach into the rear wing support stiffener, located on the ceiling behind the co-pilot location. All belts were tightened to a pretension of approximately 20 lb. Figure 14 shows the occupant configuration, prior to the test.

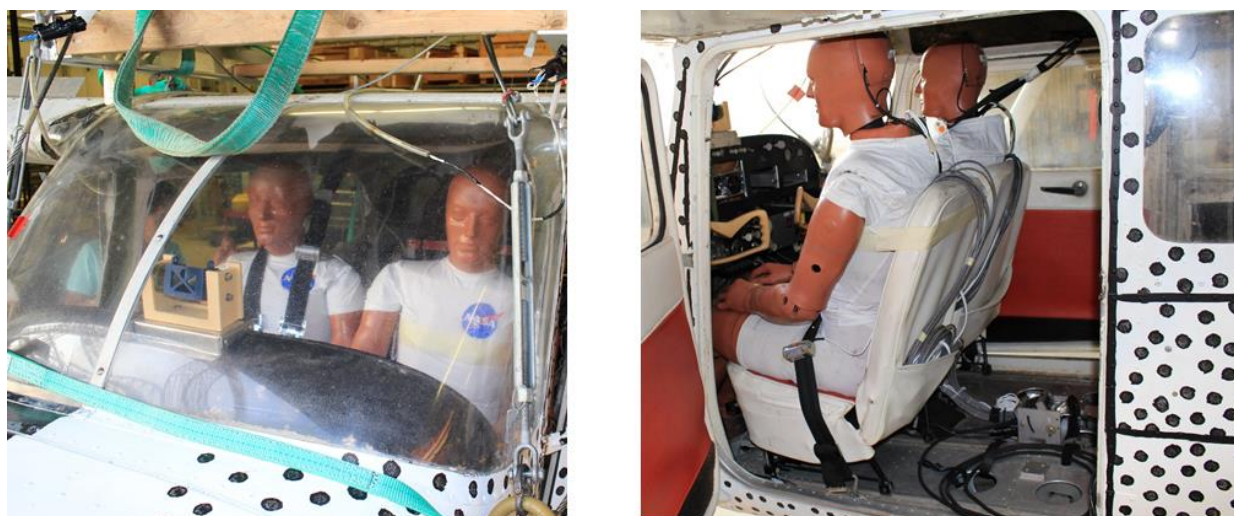


Figure 14 - Test 2 occupant configuration - pre-test

Load cells were located on the lap belt for the pilot and on the left y-harness shoulder strap for the co-pilot. The high speed camera mounted in the instrument panel was able to capture the entire impact event, starting at soil contact and ending after the airplane had flipped upside-down. Four frames of the video are presented in Figure 15. The upper left frame in Figure 15, shows the occupant position at impact. As with Test 1, the ATDs are in a symmetric configuration, sitting upright with their hands on their knees. The upper right frame shows the ATD position at the time of maximum lumbar load, which occurs just after the time of maximum vertical acceleration, but also at the time of maximum horizontal acceleration. The effect of the maximum horizontal acceleration is shown by noting that both ATDs have begun to flail forward. The lower left frame shows a major event happening: the y-harness restraint used on the co-pilot failing at the stitching location. This failure occurred at 0.137 seconds after impact, which is 0.020 seconds after the peak acceleration value measured by the co-pilot floor accelerometers, and will be discussed in detail below. Because this restraint failed, both ATD torsos flailed forward. The lower right frame



shows the maximum forward flail; however, the camera lens was not wide enough to capture the position of each of the ATDs heads at this particular time.



Figure 15 - Test 2 occupant motion sequence - onboard camera

The wing cameras were in a better position to capture the flail and are next examined. Figure 16 shows the pilot flail from the pilot wing camera. The wing camera frame clearly shows the pilot head impacting the instrument panel. Using this view, along with the timing of the instrument panel camera shows that this event occurred very early in the impact loading. It occurred immediately after the maximum horizontal acceleration, but before the airplane had started to flip over, meaning the large horizontal acceleration due to the initial impact was the cause of the head strike and not the flipping of the airplane.

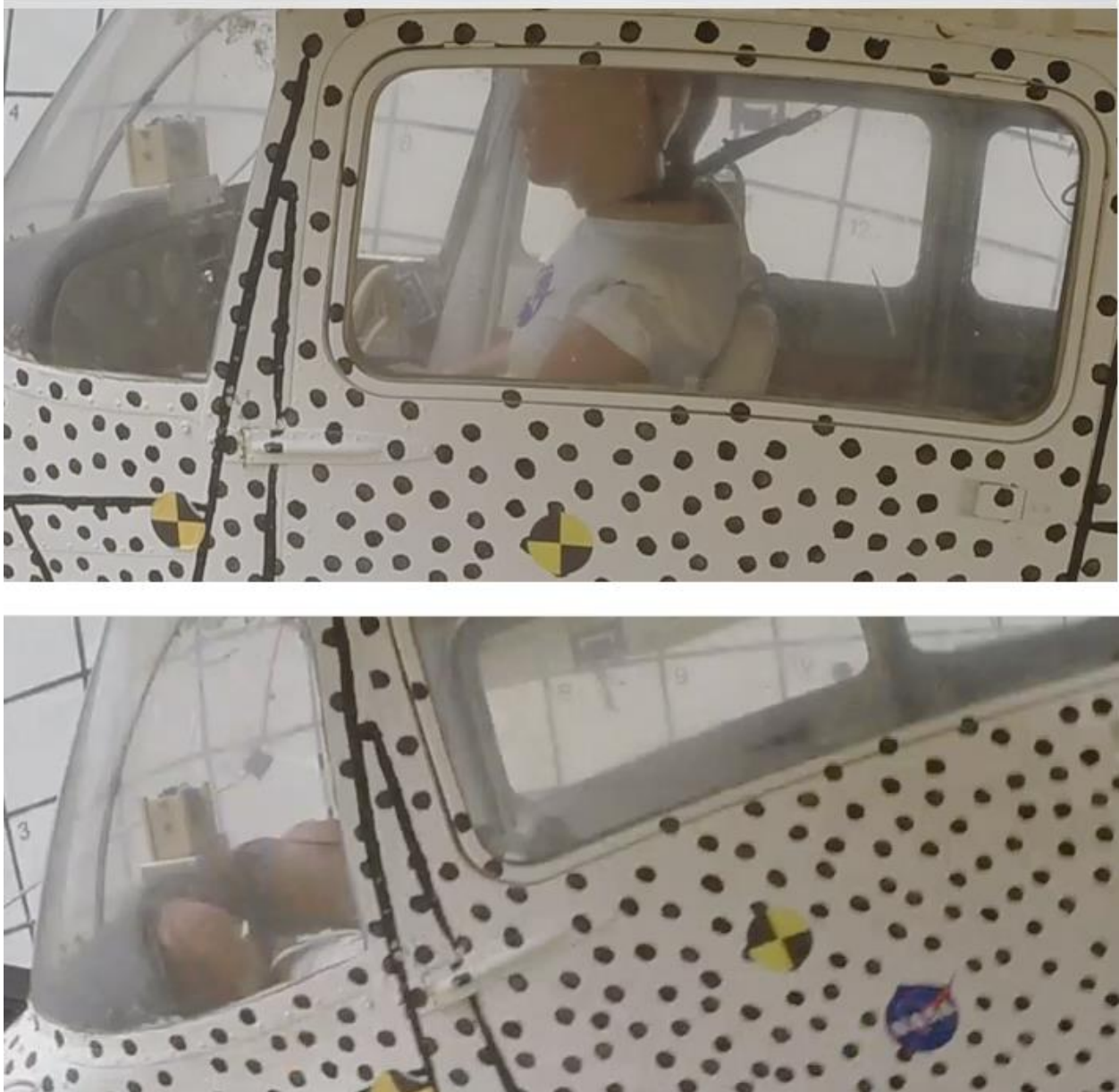


Figure 16 - Test 2 pilot head flail. Before impact (top) and max flail (bottom)

The wing camera showing the co-pilot flail was next examined, and is shown in Figure 17. A major result from Test 2 is that the y-harness restraint failed at approximately 0.137 seconds after impact. The failure occurred at the stitching where the “y” portion of the shoulder harness met with the single roof attachment strap. This failure caused the co-pilot to act much like the pilot. However, the additional restraint of the torso due to the y-harness being present (before failure) delayed the forward motion enough that the co-pilot head may have just narrowly missed striking the instrument panel, or potentially struck the instrument panel with much less force than that of the pilot. This finding will be confirmed when examining the acceleration profiles of the ATDs heads.



Figure 17 - Test 2 co-pilot head flail. Before impact (top) and max flail (bottom)

Figure 18 shows two adjacent frames of video showing the y-harness before and after failure. Post-test inspections of the y-harness showed that it failed in the stitching which connected the y-web portions meant to go over the torso to the single aircraft attachment web. The webbing itself did not fail. Note that because the load cell was measuring a single portion of the y-harness, the loads can be assumed to be double the measured value on both the stitching and aircraft attachment webbing.



Figure 18 - Test 2 y-harness failure

The strap loads are plotted in Figure 19. The load cell reading in the y-shoulder harness reaches a peak value of 570 lb., which implies the stitching failure occurred at 1140 lb. The straps immediately unload after the failure due to loss of tension, and the load cell reading goes to zero. This failure load is well below the Upper Torso Restraints Requirement of 2,500 lb., as defined in SAE “Restraint Systems for Civil Aircraft” [24]. The pilot lap belt reached a maximum load of 764 lb. The maximum forward flail for both occupants occurred after 0.200 seconds, which was a much later time than either of the strap load maximums. Had the y-harness not failed, the maximum flail for the co-pilot would have been much less. Figure 20 shows the failure of the y-harness in detail and compares to the same y-harness, when new.



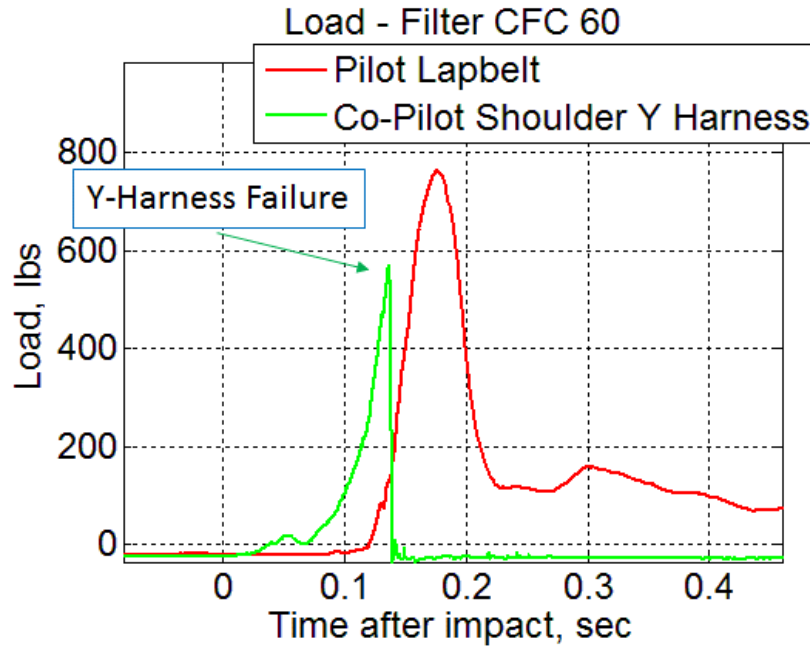


Figure 19 - Test 2 seatbelt loads



Figure 20 - Test 2 shoulder y-harness failure

Lumbar loads are next examined and plotted in Figure 21. The pilot experiences a 525 lb. maximum lumbar load 0.115 seconds after impact, while the co-pilot experiences a 587 lb. maximum lumbar load which is 0.124 seconds after impact. The pilot and co-pilot's maximum values occur at almost the same time, which is also approximately the same time as the maximum horizontal acceleration on the floor. These values are well below the 1,500 lb. FAA guideline, suggesting that injury due to spinal compression did not occur.

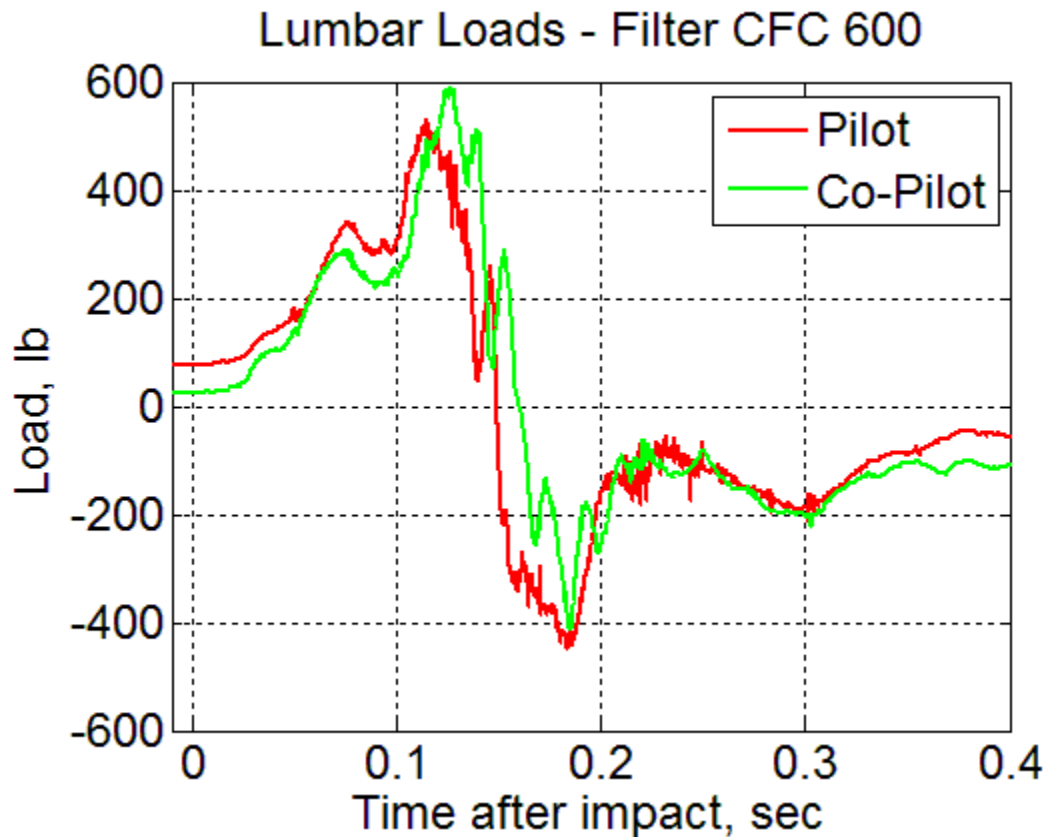


Figure 21 - Test 2 lumbar loads

The accelerations in the horizontal direction are shown in Figure 22 while the vertical accelerations are shown in Figure 23 for both the pilot and co-pilot. The pilot experiences large horizontal accelerations in the head, with a peak of 589 g (out of range in Figure 22). The large spike in the horizontal head acceleration confirms that the pilot head struck the instrument panel approximately 0.15 seconds after impact. The large chest accelerations are also a result of the pilot flail during the impact. The chest experiences 70.3 g peak acceleration. In contrast, the pelvis which is restrained by the lap belt only experiences 25.6 g peak acceleration.

These responses are contrasted by the response in the co-pilot. The head acceleration peaks at 70.0 g. While still high, the addition of the y-harness restrains it enough to not severely strike the instrument panel or yoke. The co-pilot chest acceleration achieves a 52.8 g peak, while the peak pelvic acceleration is only 23.8 g.

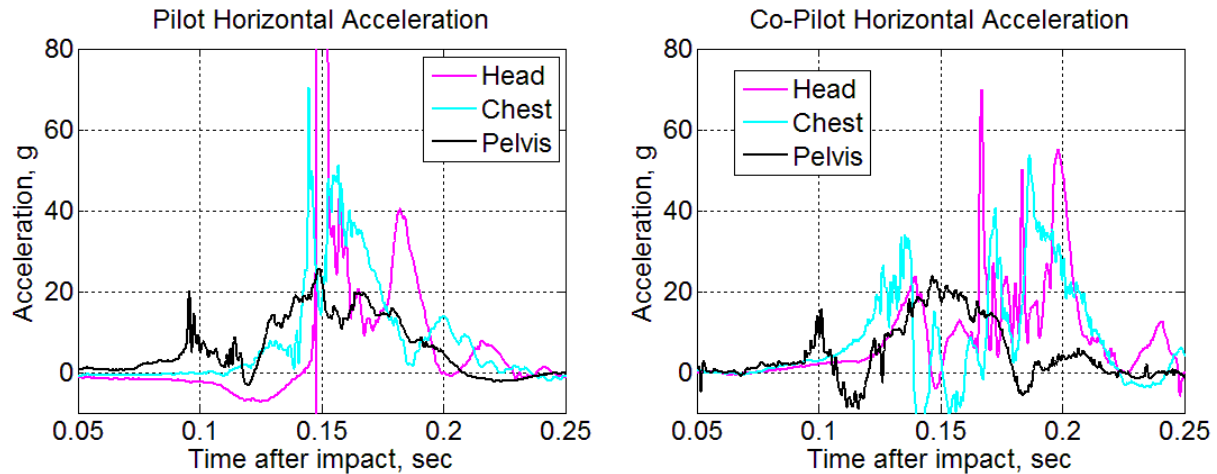


Figure 22 - Test 2 ATD horizontal acceleration. Pilot (left) and co-pilot (right)

Vertical accelerations were next examined and are shown in Figure 23. Large accelerations also show up in the vertical acceleration values in the pilot. The head experiences a short spike of 234.8 g (out of range in Figure 23), whereas the co-pilot head experiences only a 49.1 g peak acceleration. The pelvic accelerations match more closely, at 30.1 g and 28.7 g for the pilot and co-pilot, respectively. These values were then used in the HIC calculation, with the results shown in Table 3. The HIC value for the pilot is well above the established limit of 1,000. The pilot head clearly hit the instrument panel and a cranial fracture has occurred. The co-pilot, even with the spikes in the acceleration data, shows a maximum HIC below the limit of 1,000.

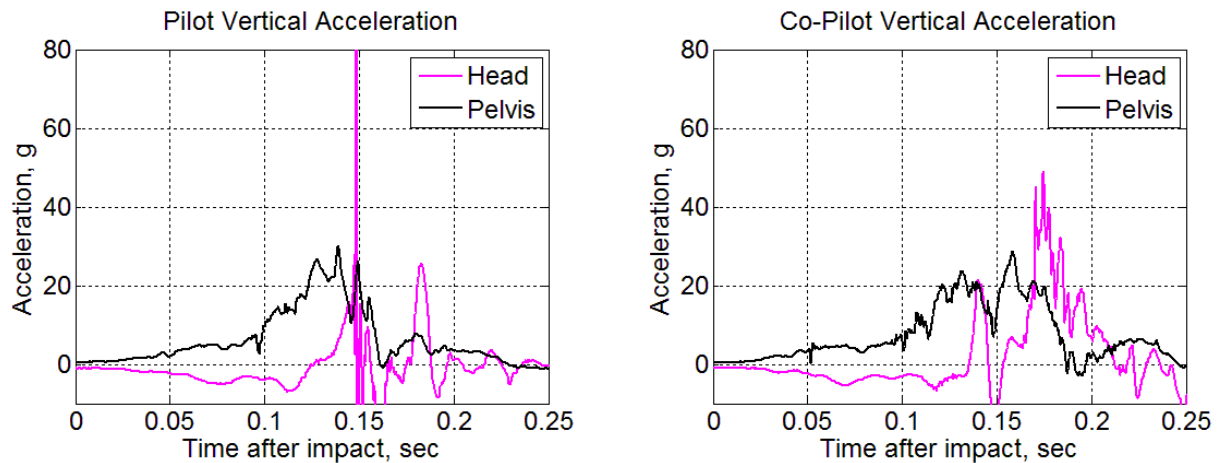


Figure 23 - Test 2 ATD vertical acceleration. Pilot (left) and co-pilot (right)

Table 3 - Test 2 HIC36 values

	HIC36
Pilot	4,241
Co-pilot	274

Additional post-test inspections were completed on the airframe once removed from the soil and set right-side-up in the preparation hangar. When the seats were examined, it was noted that both rear seat rail attachments for both seats were either partially or fully pulled out from the seat track. All four of the front seat attachments were set normally in the seat track. The rear seat attachment failure is likely due to the large amount of ATD flail due to the horizontal accelerations experienced at impact. All restraint attachments were still secure in their aircraft attachment locations. Figure 24 shows the seat pullout.

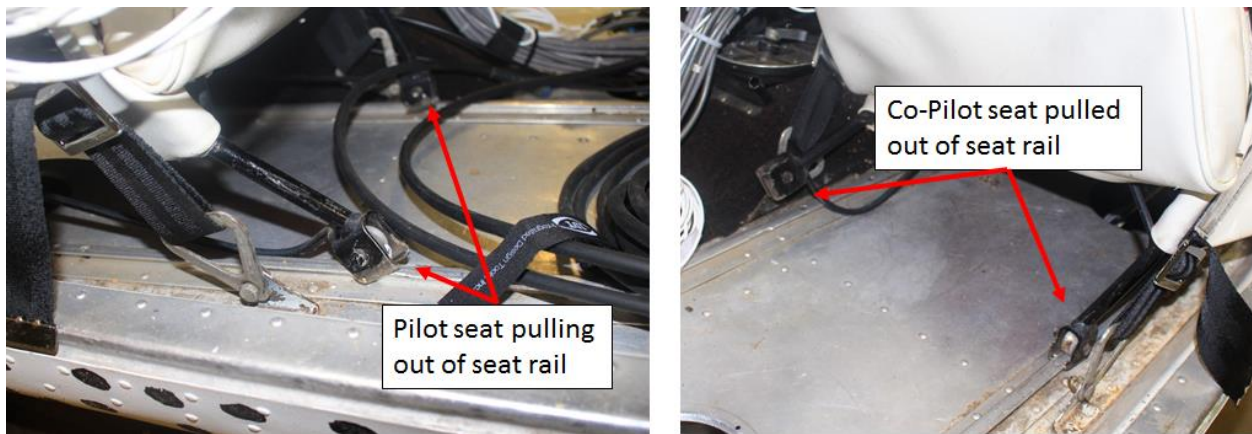


Figure 24 - Test 2 seat partial pullout

Test 2 results showed that a crash into dirt resulted in very large horizontal and vertical accelerations both on the airframe and on the occupants due to the penetration and plowing into the soil. These large accelerations occurred during the first 0.300 seconds after the impact, while the flipping of the airplane required a few seconds to complete. The results show that the sudden large horizontal accelerations are the injurious part of the crash, not the flipping and by the time the flipping has begun to occur, the maximum accelerations have already occurred and the occupants have already experienced their maximum loading.

In this test, two types of restraints were used, a lap belt only and a lap belt with y-harness. Surprisingly, the y-harness failed in the stitching at the junction between the y and the overhead attachment strap, at an estimated load of 1,140 lb. After the failure, both the pilot and co-pilot head accelerations experienced significant spikes, with the spike in the pilot head being large enough to register over the HIC limit. Even though the y-harness failed and the co-pilot likely impacted the instrument panel or yoke, the severity of the impact was much reduced due to the restraint of the y-harness, prior to failure.

### Test 3 Results

Test 3 was conducted on August 26, 2015 and was the second test where the airplane impacted a soil surface. As with the first soil test, the surface was to represent a dirt field or other type of unprepared surface not considered rigid.

The pilot was outfitted with a shoulder and lap belt. The co-pilot was outfitted with a shoulder belt with inertia reel and lap belt. Both restraints were purchased new and outfitted into the existing restraint attachment points. The pilot belts were tightened to a pretension of approximately 20 lb. The co-pilot lap belt was also pretensioned to 20 lb.; however, the characteristics of the inertia reel disallowed for pretensioning. Figure 25 shows the occupant configuration, prior to the test.

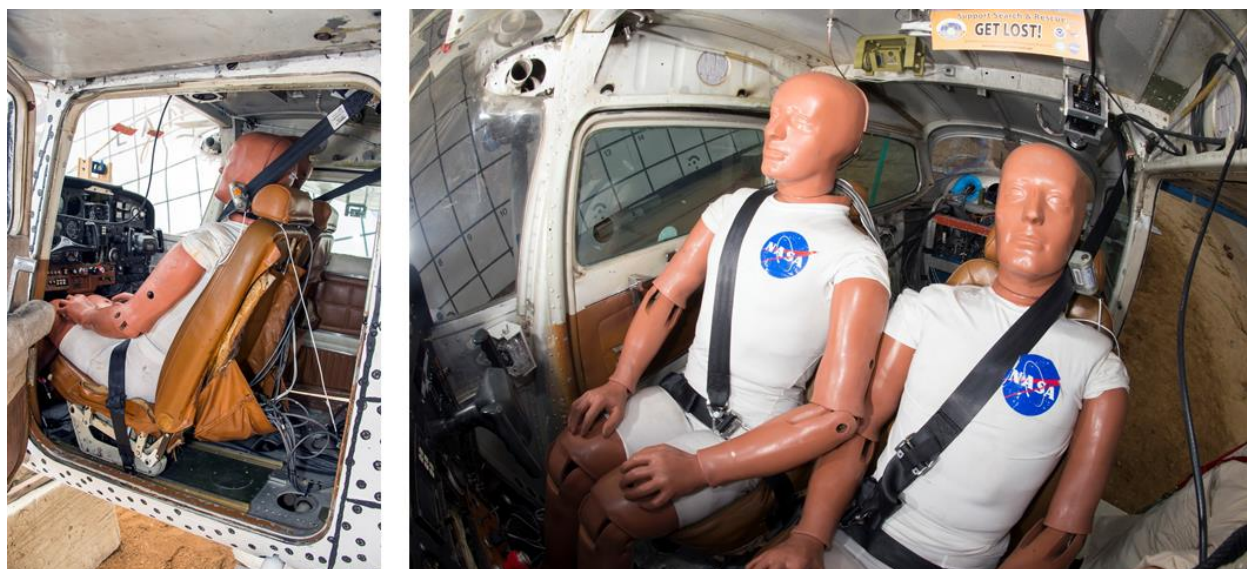


Figure 25 - Test 3 occupant configuration - pre-test

The airplane CG impacted the soil at a 56.9-ft./sec. horizontal and 23.6-ft./sec. vertical velocities. The AoA was 8.0 degrees nose up with a pitch rate of +13.3 degrees/second. Test 3 included a slight amount of roll (right side high) and yaw (nose left).

Due to the slight amount of roll and yaw, the airplane left main gear impacted the soil first. Shortly thereafter, the tail contacted the surface at 0.030 seconds after impact. The tail contact created a slap down effect where a significant amount of nose down rotation occurred at a pivot point on the tail. This slap down effect caused the nose gear, along with the nose of the airplane to contact the soil 0.116 seconds after impact. As with Test 2, after the nose gear penetrated into the soil surface, the airplane started to flip around the nose, which acted like a pivot point. Unlike Test 2, however, the tail developed a fracture aft of station 108 at 0.138 seconds after impact. This fracture caused the tail to peel away from the fuselage, acting much like a hinge. A small portion of skin on the bottom of the aircraft retained the tail to the rest of the airplane during the rotation. The rotation of the aircraft lasted until approximately 1.53 seconds after impact, at which time the ceiling of



the airplane contacted the soil. The airplane rocked for a few seconds before finally coming to rest at almost 5 seconds after initial impact. The post-test configuration of the airplane in Test 3 is shown in Figure 26.



Figure 26 - Post-test orientation of airplane in Test 3

The accelerations on the floor beneath the pilot and co-pilot seats are plotted in Figure 27. As in Test 2, the acceleration experienced in the airplane from the ground (soil) contact occurred within the first 0.300 seconds of impact, both in the horizontal and vertical directions. Accelerations were very symmetric between the pilot and co-pilot position, suggesting the roll and yaw did not adversely affect the acceleration on the floor. The horizontal acceleration resembles generally a triangular shape, but contains a small plateau at the beginning of the pulse, due to the initial penetration of the gear into the soil. Maximum accelerations were -18.1 g for the pilot and -17.6 g for the co-pilot. These maximums occurred at 0.163 seconds after impact. The two acceleration curves closely mimicked each other.

In the vertical direction, the accelerations represented a plateau shape with spikes occurring 0.160 seconds and 0.195 seconds after impact. The peak accelerations reach 17.9 g for the floor under the pilot and 15.7 g for the floor under the co-pilot. The pulse duration lasts approximately 0.295 sec. Average accelerations, which occur between 0.100 seconds and 0.200 seconds, are 8.3 g for the pilot and 7.7 g for the co-pilot.

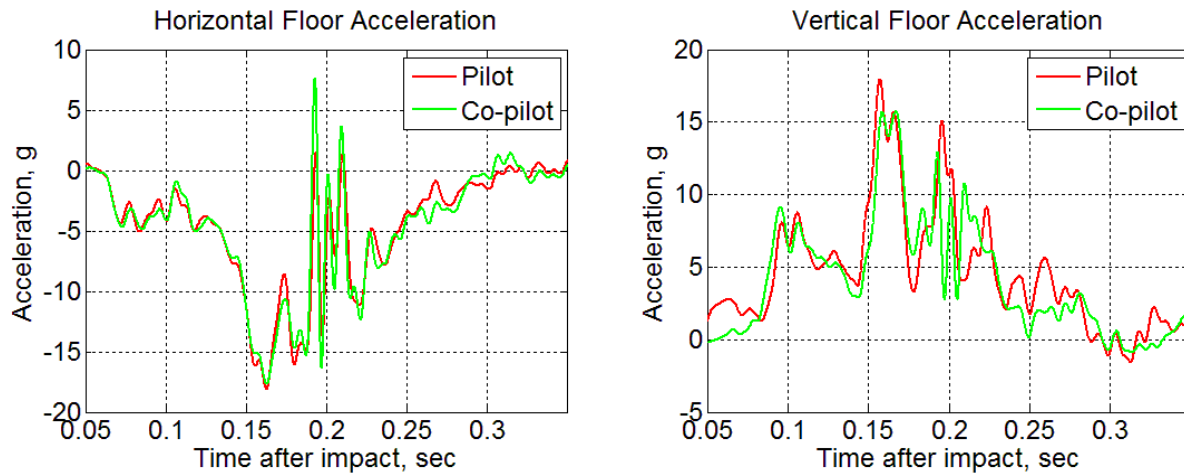


Figure 27 - Floor accelerations from Test 3

An onboard camera, mounted in the instrument panel, captured the ATD motion throughout the entire crash sequence. Individual frames showing notable events were extracted from the video, and are presented in Figure 28. Airplanes used in Tests 1 and 2 did not have armrests on the doors. The armrests on the doors of the Test 3 airplane obstructed the positioning of the elbows; therefore, the ATDs had to be offset in order to fit in the cabin. The upper left picture shows the co-pilot left arm sitting slightly overlapping the pilot arm. Similar to Test 2, the maximum load in the co-pilot lumbar region is very early in the impact event, occurring at 0.130 seconds after impact. At this point, due to the co-pilot initial position, the co-pilot has started rotating about the shoulder restraint causing the head to lean toward the pilot position. The upper right image shows the pilot at the time of maximum lumbar loading which occurs slightly later in the impact event at 0.175 seconds. At this point, the co-pilot head has started to point straight forward. At 0.200 seconds after impact, the maximum loads developed in the shoulder restraint occurred both for the pilot and co-pilot. The bottom middle image shows both occupants seated normally while the airplane was flipping over, and this image was taken when it had achieved a vertical orientation. The bottom right picture shows the occupants, post-test, with their hands out pointing toward the ground, and in a symmetric configuration. The wing cameras were next examined to show maximum flail in the pilot and co-pilot.



Figure 28 - Test 3 occupant motion sequence - onboard camera

The image series of the pilot taken from the wing camera is shown in Figure 29. Using the best available scaling information based on the window dimensions, the maximum flail encountered in the head of the pilot was 7.27 in. in the forward direction. However, the pilot was never in danger of striking either the yoke or the instrument panel, even with the rotation and flipping over of the airplane.





Figure 29 - Test 3 pilot head flail. Before impact (top) and max flail (bottom)

The co-pilot flail was next examined and is shown in Figure 30. Using the best available scaling information based on the window dimensions, the maximum flail encountered in the head of the co-pilot was 12.5 in. in the forward direction, which was approximately 5.25 in. more than the pilot.



Figure 30 - Test 3 co-pilot head flail. Before impact (top) and max flail (bottom)

Restraint loads were next examined. Even with the large rotation in the co-pilot, the inertia reel three-point restraint kept the head from striking any portion of the instrument panel and/or yoke. Due to the restraint of this large rotation, the maximum belt load in the inertia reel was 1,144 lb. and occurred approximately 0.2 seconds after impact, and more specifically at the time of maximum co-pilot torso flail. The maximum pilot harness load was 981 lb. and occurred a short time later at 0.215 seconds after impact. The restraint anchoring points, both on the floor and on the wall behind the doors showed no signs of failure for either the pilot or co-pilot. Figure 31 shows the time history of the restraint loading.

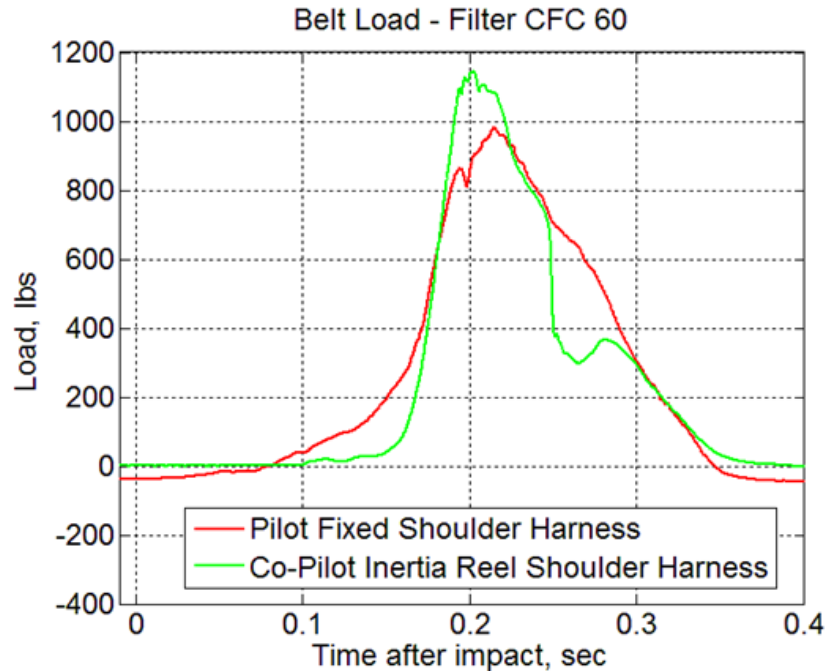


Figure 31 - Test 3 seatbelt loads

ATD data were next examined, and lumbar load forces are plotted in Figure 32. Lumbar loads for the pilot and co-pilot reached similar peak values, and both responses had similar double peak shapes. However, the timing of the peak values was reversed between the pilot and co-pilot; showing up as the first peak for the co-pilot and the second peak for the pilot. The co-pilot also had a sharper rise and falling time as compared to the pilot; however, the majority of the loading was complete at approximately 0.3 seconds after impact. The peak value for the pilot was approximately 923 lb. and occurred at 0.176 seconds after impact, while the peak value for the co-pilot was 956 and occurred 0.128 seconds after impact. It is hypothesized that, because shoulders of the ATDs were overlapping slightly prior to and during the first stages of the crash sequence, the shifting of the ATDs during the crash caused the double peaks. Neither of these values, however, reached the FAA spinal injury threshold of 1,500 lb., indicating that spinal compression injury did not occur.

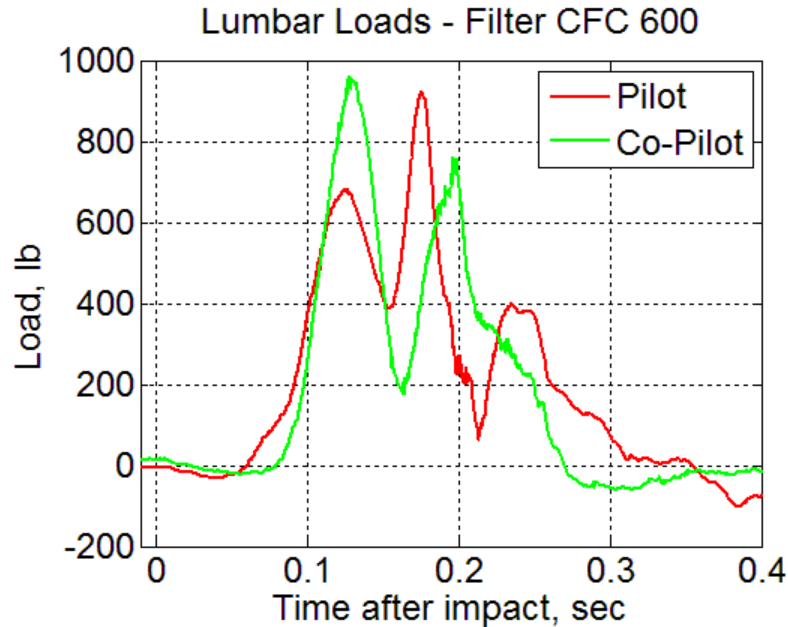


Figure 32 – Test 3 lumbar loads

Accelerations from both the pilot and co-pilot were next examined. Figure 33 shows the accelerations measured in the horizontal direction. In general, the pilot and co-pilot horizontal accelerations match in shape and duration. The pilot horizontal head acceleration reaches a peak value of 19.2 g while the co-pilot reaches a peak horizontal acceleration of only approximately 14.5 g. Both of these events occur approximately 0.25 seconds after impact. The co-pilot experiences a short duration spike in acceleration, which occurs approximately 0.3 seconds after impact, and reaches a peak value of -52.7 g. Since the head did not physically contact with any obstacle, the spike is likely due an electrical anomaly. Similarly, the chest and pelvic accelerations also matched generally in shape and duration. The co-pilot experienced a slight amount of increased acceleration, presumably due to the large amounts of rotation about the shoulder harness.

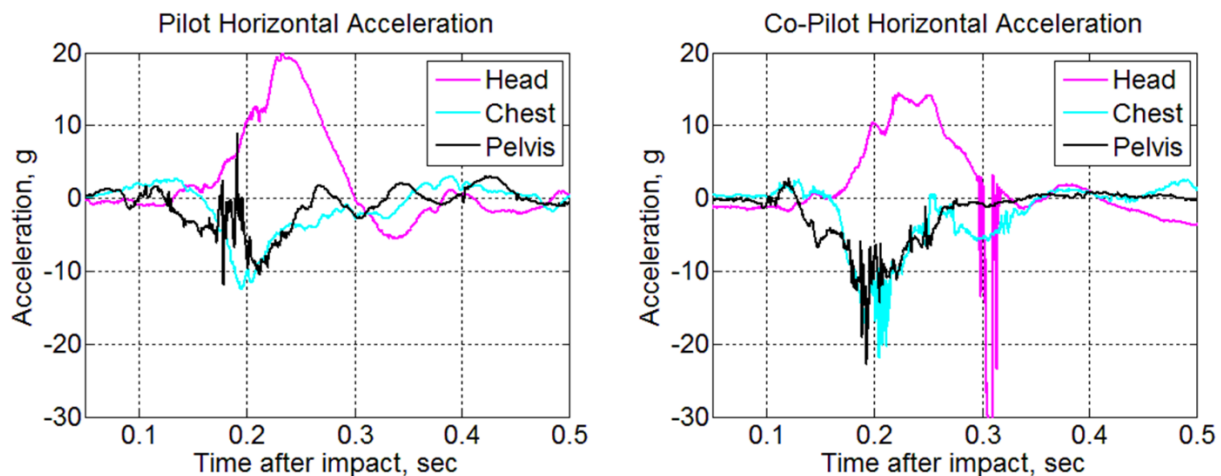


Figure 33 - Test 3 ATD horizontal acceleration. Pilot (left) and co-pilot (right)

Vertical accelerations were next examined, and are shown in Figure 34. The pilot and co-pilot also experienced similar vertical magnitudes and shapes, with the notable exception of the head of the co-pilot. Due to the large amounts of rotation of the co-pilot head and torso around the shoulder harness, the head reaches a maximum acceleration of -25.7 g at approximately 0.22 seconds after impact, which is near the time of maximum belt load and also maximum flail. The pilot, in contrast, only experiences a maximum acceleration of -9.9 g. The pelvic vertical accelerations were almost identical both in shape and magnitude, reaching peaks of 18.5 g and 18.0 g for the pilot and co-pilot, respectively. These numbers were then used for the HIC computation, which is shown in Table 4. Because neither the pilot nor co-pilot head impacted either the instrument panel or yoke, the HIC limits for Test 3 were well below the established limits of 1,000.

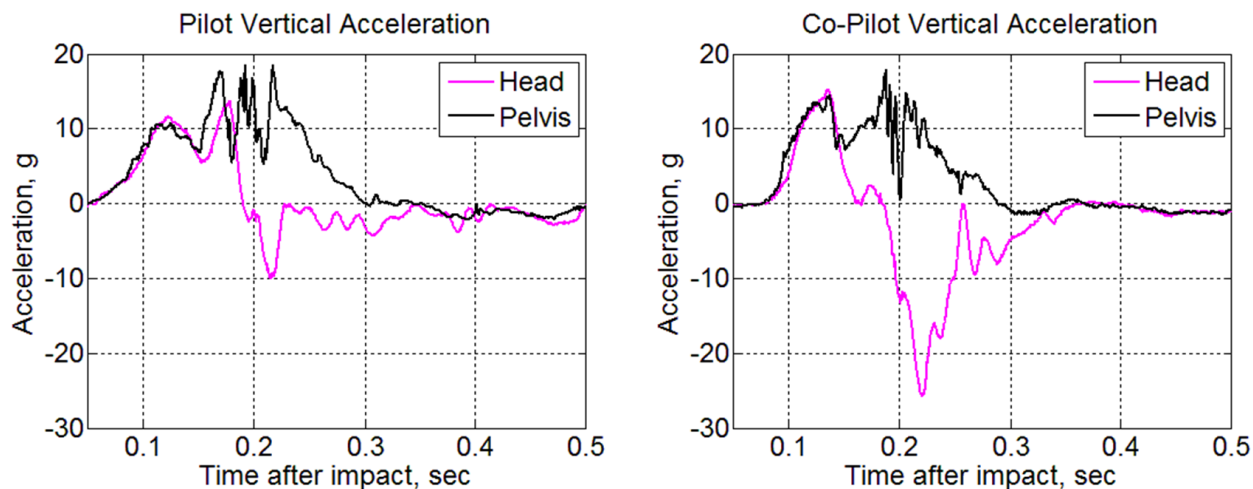


Figure 34 - Test 3 ATD vertical acceleration. Pilot (left) and co-pilot (right)

Table 4 - Test 3 HIC36 values

	HIC36
Pilot	51
Co-pilot	92

Similarly to Test 2, the aircraft experienced a large amount of rotation due to it flipping over at impact. The chair rails were examined for signs of pull out or failure. The co-pilot chair was pulled out on the rear outboard leg, and cracking was evident in the rail itself. The pilot seat fared much better with no signs of pullout or seat rail cracking. The pullout in the co-pilot chair is presumably due to the large amount of forward motion experienced in the co-pilot. The pilot, in contrast, did not experience significant motion. A picture of the co-pilot rear outboard leg taken at the impact location immediately after Test 3 is shown in Figure 35.



Figure 35 - Test 3 co-pilot seat pullout

Test 3 results showed that a crash into dirt in a tail strike condition can also result in the airplane flipping over and landing upside down. As with Test 2, the dirt contact resulted in very large horizontal and vertical accelerations both on the airframe and on the occupants due to the sudden stopping of the airplane at the impact location. And similarly, these large accelerations occurred during the first 0.300 seconds after the impact, while the flipping of the airplane required a few seconds to complete. The resultant high accelerations experienced in the pilot and co-pilot were mainly due to loading during the first 0.300 of impact, and not due to the flipping action of the aircraft.

Since both ATDs were restrained with 3 point harnesses, the resultant injury metrics all showed a low probability of injury. The space issues inside the cockpit required offsetting the ATDs, such that part of their elbows overlapped in the middle. This overlapping caused the co-pilot ATD to rotate about the shoulder harness; however, the co-pilot did not end up striking either the instrument panel or yoke. Both ATDs remained seated even after the impact even when the aircraft was oriented upside-down post-test.

## Discussion

Test 1 resulted in a dual impact scenario. The first impact was dominated by the airplane impacting the rigid surface with a large sink rate, and represented a stall-to-emergency or crash landing. This impact gave the highest vertical accelerations in the ATDs and airframe. It was also during this impact that the lumbar loads reached their highest values; however, they did not come close to exceeding the limit established by the FAA. The second impact was a result of a safety net stopping the residual horizontal velocity of the aircraft and represented the airplane impacting a soft obstruction during rollout from the initial ground impact. It was during the second impact that both airframe and ATD horizontal accelerations were the highest. The horizontal accelerations were not severe enough to cause either the pilot or co-pilot's head to strike the instrument panel or yoke.



However, for the co-pilot outfitted only with a lap belt, the onboard video data show that the head came very close to striking the instrument panel. If the aircraft had landed at a slightly higher velocity, or experienced a slightly shorter deceleration pulse duration, the co-pilot would have experienced a head strike scenario and the potential for injury would have greatly increased. The airframe itself was mostly undamaged.

Test 2 was the first of the soil impact tests and was a good representation of a CFIT scenario. The airplane impacted the surface nose first at a 12.2 degrees nose down angle. The pilot, which was only restrained by a lap belt, experienced severe injury when the head hit the instrument panel, due to the large amount of torso motion. The co-pilot, restrained by a y-harness restraint did not strike the instrument panel hard enough to register an injury using the HIC metrics, even after the y-harness failure.

In Test 3, the airplane impacted the ground in a nose up configuration, which was the opposite configuration as Test 2. However, the final result of Test 3 was very similar to Test 2. Both airplanes sunk into the dirt and both airplanes flipped over and landed upside down near the original impact location. The onboard occupant responses are different; however, because in Test 3 both occupants were restrained with 3 point harnesses, the results showed the pilot survived in Test 3, which is in contrast to Test 2.

The occupant data suggest that the three crashes are severe but survivable by strictly using the various forms of injury criteria presented; however, it should be noted that there are other human factors affecting each individual which may lead to injuries sustained during what is considered a survivable crash. There are also measurable injury metrics that were unable to be performed due to data constraints. Thus, for example, there could have been potential for broken arms or legs during any one of the crash tests presented. If broken leg(s) were to occur, it is unlikely that the occupant would be able to egress the aircraft and travel any significant distance to obtain help.

## **Conclusion**

The three Cessna 172 crash tests conducted and documented in this report recreated three types of airplane accidents in which the occupants experienced a severe but survivable loading condition. The impact conditions themselves were very different in nature; however, the last two tests resulted in similar post-impact kinematics. Maximum accelerations for all three tests did not exceed 30 g when measured at the seat interface locations.

The three tests gave the opportunity to evaluate four types of restraints under three types of loading conditions. The restraints tested were a lap belt, a lap belt with shoulder harness, a lap belt with y-harness, and a lap belt with shoulder harness and inertia reel. The results reinforce the previous guidance from the FAA and others that a three point harness provides much benefit when keeping the occupant restrained in a crash event.

Any of the three point harnesses proved to be beneficial when comparing the occupant flail and loads to the lap belt only occupant. Even the failed three point harness in Test 2 still restrained the

co-pilot from severely striking the yoke or instrument panel, saving what could have been a cranial fracture. In Tests 2 and 3, there were clear signs of seat rail failures and seat pullout. These failures were mainly due to the large amount of forward flail of the occupants compounded with the rotation of the airplane during the test.

It is hoped that the data presented offer further insight into the dynamics which occur during GA crash events and will lead to improved understanding of the airframe-seat-occupant-restraint coupling. While the test series consisted of only three crash scenarios and four restraint types, it is hoped that these results are beneficial for continued studies of GA crashworthiness and occupant protection.

## **Acknowledgements**

This research was funded by NASA Search and Rescue (SAR) Mission Office located at Goddard Space Flight Center in Greenbelt, MD. Thanks to all SAR management for their support and all of the engineers and technicians at the NASA LandIR facility for working with the utmost competence and efficiency to achieve three successful tests in a short timeframe.

## **References**

1. Littell, J.D. and Stimson, C.M. "Emergency Locator Transmitter System Performance from Three Full Scale General Aviation Crash Tests." NASA TM-2016. In Publication.
2. Vaughn, V.L. and Alfaro-Bou, E. "Impact Dynamics Research Facility for Full-Scale Aircraft Crash Testing." NASA TN, TN D-8179, April 1976.
3. Federal Aviation Administration. "Dynamic Test of Part 23 Airplane Seat/Restraint Systems and Occupant Protection." FAA AC 23.562-1. June 22, 1989.
4. National Aeronautics and Space Administration. "NASA Helps Create a Parachute to Save Lives, Planes." <http://www.nasa.gov/centers/langley/news/releases/2002/02-087.html>. Accessed Oct 20, 2015.
5. Jackson, K.E., Kellas, S., Horta, L.G., Annett, M.S., Polanco, M.A., Littell, J.D. and Fasanella, E.L. "Experimental and Analytical Evaluation of a Composite Honeycomb Deployable Energy Absorber." NASA TM-2011-217301. November 2011.
6. National Transportation and Safety Board. "Safety Report – General Aviation Crashworthiness Project: Phase 3 – Acceleration Loads and Velocity Changes of Survivable General Aviation Accidents." PG85-917016. September 1985.
7. National Transportation and Safety Board. "Annual Review of Aircraft Accident Data U.S. General Aviation, Calendar Year 2002." NTSB/ARG-06/02. November 2006.



8. Federal Aviation Administration. "Special Retroactive Requirements." FAR Part 23, Section 2. Amended August 15, 1988.
9. Li, G, and S.P Baker. "Crashes of Commuter Aircraft and Air Taxis. What determines pilot survival?" J. Occupation Medicine. Dec 1993. 35 (12). Pp. 1244-1249.
10. Federal Aviation Administration. "Seat Belts and Shoulder Harnesses: Smart Protection in Small Airplanes." FAA Brochure. AM-400-90/2.
11. Transport Canada. "Use of Safety Belts and Shoulder Harnesses on Board Aircraft." AC 605-004. November 2014.
12. National Transportation and Safety Board. "Airbag Performance in General Aviation Restraint Systems." NTSB/SS-11/01. January 2011.
13. Annett, M.S., Littell, J.D., Jackson, K.E., Bark, L.W., DeWeese, R.L. and McEntire, B.J. "Evaluation of the First Transport Rotorcraft Airframe Crash Testbed (TRACT 1) Full-Scale Crash Test." NASA TM-2014-218543. October 2014.
14. Annett, M.S., and Littell, J.D. "Evaluation of the Second Transport Rotorcraft Airframe Crash Testbed (TRACT 2) Full Scale Crash Test." Proceedings from the AHS 71<sup>st</sup> Annual Forum, Virginia Beach, Virginia. May 5-7, 2015.
15. Jackson, K.E., Fasanella, E.L., Boitnott, R.L., McEntire, B.J. and Lewis, A. "Occupant Responses in a Full-Scale Crash Test of the Sikorsky ACAP Helicopter." NASA TM 2002-211733. June 2002.
16. Littell, J.D. "Full Scale Crash Test of a MD-500 Helicopter." Proceedings from the AHS 67<sup>th</sup> Annual Forum, Virginia Beach, Virginia. May 3-5, 2011.
17. Jones, L.E. and Carden, H.D. "Overview of Structural and Occupant Responses from a Crash Test of a Composite Airplane." NASA TM 111951. 1995.
18. Littell, J.D. "Experimental Photogrammetric Techniques used on Five Full Scale Aircraft Crash Tests." NASA TM-219168. March 2016
19. Society of Automotive Engineers. "Surface Vehicle Recommended Practice: Instrumentation for Impact Test-Part 1- Electronic Instrumentation." SAE J211-1, July 2007.
20. Littell, J.D. "Crash Test of Three Cessna 172 Aircraft at NASA Langly Research Center's Landing and Impact Research Facility." NASA TM-2015-218987. November 2015.
21. U.S Dept. of Transportation. "Occupant Crash Protection." Federal Motor Vehicle Safety Standard No. 208.

22. Schmitt, K.-U., Niederer, P. and Walz, F. "Trauma Biomechanics: Introduction to Accidental Injury." Verlag Berlin Heidelberg New York: Springer, 2004.
23. Federal Aviation Administration. "Emergency Landing Dynamic Conditions." FAR Part 23, Section 562. Amended Feb. 9, 1996.
24. Society of Automotive Engineers. "Restraint Systems for Civil Aircraft." SAE-AS8043 Rev B. March 2013.

REPORT DOCUMENTATION PAGE					Form Approved OMB No. 0704-0188	
<p>The public reporting burden for this collection of information is estimated to average 1 hour per response, including the time for reviewing instructions, searching existing data sources, gathering and maintaining the data needed, and completing and reviewing the collection of information. Send comments regarding this burden estimate or any other aspect of this collection of information, including suggestions for reducing this burden, to Department of Defense, Washington Headquarters Services, Directorate for Information Operations and Reports (0704-0188), 1215 Jefferson Davis Highway, Suite 1204, Arlington, VA 22202-4302. Respondents should be aware that notwithstanding any other provision of law, no person shall be subject to any penalty for failing to comply with a collection of information if it does not display a currently valid OMB control number.</p> <p><b>PLEASE DO NOT RETURN YOUR FORM TO THE ABOVE ADDRESS.</b></p>						
1. REPORT DATE (DD-MM-YYYY)		2. REPORT TYPE			3. DATES COVERED (From - To)	
01-03 - 2016		Technical Memorandum				
4. TITLE AND SUBTITLE  ATD Occupant Responses from Three Full-Scale General Aviation Crash Tests				5a. CONTRACT NUMBER		
				5b. GRANT NUMBER		
				5c. PROGRAM ELEMENT NUMBER		
6. AUTHOR(S)  Littell, Justin D.; Annett, Martin S.				5d. PROJECT NUMBER		
				5e. TASK NUMBER		
				5f. WORK UNIT NUMBER  736466.01.08.07.55.01		
7. PERFORMING ORGANIZATION NAME(S) AND ADDRESS(ES)  NASA Langley Research Center Hampton, VA 23681-2199				8. PERFORMING ORGANIZATION REPORT NUMBER  L-20674		
9. SPONSORING/MONITORING AGENCY NAME(S) AND ADDRESS(ES)  National Aeronautics and Space Administration Washington, DC 20546-0001				10. SPONSOR/MONITOR'S ACRONYM(S)  NASA		
				11. SPONSOR/MONITOR'S REPORT NUMBER(S)  NASA-TM-2016-219175		
12. DISTRIBUTION/AVAILABILITY STATEMENT Unclassified - Unlimited Subject Category 39 Availability: NASA STI Program (757) 864-9658						
13. SUPPLEMENTARY NOTES						
14. ABSTRACT  During the summer of 2015, three Cessna 172 General Aviation (GA) aircraft were crash tested at the Landing and Impact Research (LandIR) Facility at NASA Langley Research Center (LaRC). Three different crash scenarios were represented. The first test simulated a flare-to-stall emergency or hard landing onto a rigid surface such as a road or runway. The second test simulated a controlled flight into terrain with a nose down pitch of the aircraft, and the third test simulated a controlled flight into terrain with an attempt to unsuccessfully recover the aircraft immediately prior to impact, resulting in a tail strike condition. An on-board data acquisition system (DAS) captured 64 channels of airframe acceleration, along with accelerations and loads in two onboard Hybrid II 50th percentile Anthropomorphic Test Devices (ATDs) representing the pilot and co-pilot. Each of the three tests contained different airframe loading conditions and different types of restraints for both the pilot and co-pilot ATDs. The results show large differences in occupant response and restraint performance with varying likelihoods of occupant injury.						
15. SUBJECT TERMS  Airplane testing; Anthropomorphic Test device; Full scale crash testing; Impact testing; Occupant injury; Survivability						
16. SECURITY CLASSIFICATION OF:			17. LIMITATION OF ABSTRACT	18. NUMBER OF PAGES	19a. NAME OF RESPONSIBLE PERSON	
a. REPORT	b. ABSTRACT	c. THIS PAGE			STI Help Desk (email: help@sti.nasa.gov)	
U	U	U	UU	43	19b. TELEPHONE NUMBER (Include area code)  (757) 864-9658	